

# Heart Rate Turbulence Denoising Using Support Vector Machines

JL Rojo-Álvarez, *Member, IEEE*, O Barquero-Pérez, I Mora-Jiménez, E Everss, A.B. Rodríguez-González, A García-Alberola

**Abstract**—Heart Rate Turbulence (HRT) is the transient acceleration and subsequent deceleration of the heart rate after a premature ventricular complex (PVC), and it has been shown to be a strong risk stratification criterion in patients with cardiac disease. In order to reduce the noise level of the HRT signal, conventional measurements of HRT use a patient-averaged template of post-PVC tachograms (PPT), hence providing with long-term HRT indices. We hypothesize that the reduction of the noise level at each isolated PPT, using signal processing techniques, will allow to estimate short-term HRT indices. Accordingly, its application could be extended to patients with reduced number of available PPT. In this paper, several HRT denoising procedures are proposed and tested, with special attention to Support Vector Machine (SVM) estimation, as this is a robust algorithm that allows us to deal with few available time samples in the PPT. Pacing stimulated HRT during electrophysiological study are used as a low noise gold-standard. Measurements in a 24 hour-Holter patient database reveal a significant reduction in the bias and in the variance of HRT measurements. We conclude that SVM denoising yields short-term HRT measurements and improves the signal to noise level of long-term HRT measurements.

**Index Terms**—Heart Rate Turbulence, Denoising, Short-Term, Support Vector Machine, Bootstrap Resampling,  $\epsilon$ -Huber cost, Turbulence Slope.

## I. INTRODUCTION

Heart Rate Turbulence (HRT) has been defined as the behavior of the Heart Rate (HR) after a Premature Ventricular Complex (PVC). Under normal and healthy conditions, HRT consists of a brief increase in HR after the PVC, that is immediately followed by a slower decrease in HR. Measurements on HRT characteristics in long-term (24 hour) Holter recordings have shown a high predictive power for identifying patients with high-risk of cardiac disease [1], [2]. The two parameters that have been mostly used for measuring HRT are the Turbulence Onset (TO) and the Turbulence Slope (TS), though other parameters have been also proposed [2], [3]. The TO measures the amount of sinus acceleration that follows immediately a PVC, and it is defined as the shortening of the interval average for the two sinus beats (normal-to-normal, NN) after the compensatory pause. The TO is calculated as the percentage of the two NN interval average preceding the PVC. The TS is an indicator of the amount of sinus deceleration

following the PVC, and it is usually calculated by first fitting the linear regression for each 5 consecutive NN intervals in the post-PVC tachogram (PPT) during 15 beats, and then selecting the maximum slope among all the regression lines fitted along the PPT. An important requirement for obtaining reliable HRT measurements is the adequate selection of the PPT that are useful, and a set of conditions for inclusion in the analysis have been clearly established in the literature [2]. Aiming to reduce the strongly present physiological noise of different kinds in each PPT, a PPT template is first build in each patient by averaging the set of available single PPT, and then, TS is calculated on this template. Given that the PPT template is usually averaged for 24-hour Holter recordings, indices obtained from this template are a long-term measurement of the global state of the patient during a day, and this processing has been shown to be a powerful risk stratifier not only for acute myocardial infarction [1], but also for other diseases such as Chagas [4] or heart failure [5].

Nevertheless, relevant information could be masked by the long-term averaging in this calculation procedure, both from a clinical and from a signal analysis points of view. First, relevant short-time fluctuations in the TS along the day [6] could be hidden by the 24-hour template averaging. Second, several influences of the physiological state can affect the HRT, such as the described effect of HR level that precedes to the PVC on the HRT oscillation amplitude [3], [7]. More specifically, the vegetative tone is probably controlling both the HR level and the HRT oscillation amplitude, but nevertheless, averaging along the different states during the day could result in a reduction of the true magnitude of the HRT fluctuation and in a smoothing not only in noise level, but also in signal level [6], [8]. And third, averaging precludes the comparison of HRT in a given moment to other fluctuating physiological variables. For instance, comparison of long-term Heart Rate Variability (HRV) to long term HRT has been reported [9], but the short-term regulation of the autonomous nervous system on HR can not be studied jointly with the HRT.

Therefore, our hypothesis is that efficient cancelation of physiological noise from each isolated PPT will allow the short-term quantification of TS. This would allow us also to measure the HRT in a higher number of patients, beyond the current limits given by the exclusion criteria for TS averaging with a minimum number of available PPT. Accordingly, a signal processing method capable of canceling the noise in a single PPT will be a valuable tool to evaluate the short-term HRT, and the development of such method is the purpose of this paper. Two main technical issues appear when addressing

JLRA, OBP, IMJ, EE, and ABRG, are with Department of Signal Theory and Communications, University Rey Juan Carlos (Spain). AGA is with Arrhythmia Unit, Hospital Virgen de la Arrixaca of Murcia (Spain). Address for correspondence: JL Rojo-Álvarez (*jose Luis.rojo@urjc.es*), B-004, Universidad Rey Juan Carlos, Camino del Molino s/n, Fuenlabrada-28943, Madrid (Spain). This work has been partially supported by Research Project TEC2007-68096-C02/TCM from Spanish Government and by Research Grant from Medtronic.

the signal denoising of a single PPT. First, the PPT has a very short duration (current recommendation is 15 NN samples), and hence, a very robust signal processing method will be required. Second, the HRT is usually measured from 24-hour Holter recordings, which are surely influenced by a variety of noise sources, including the daily activity and the changes in the physiological state of the patient. But a clear gold-standard for HRT behavior and measurement will be needed if we want to benchmark and compare the performance of any proposed denoising algorithm.

To overcome the first issue, we propose the use of Support Vector Machines (SVM), in particular, the SVM regressor [10]. The SVM framework has been shown specially advantageous in problems with few samples available, due to their excellent generalization performance. We will show that the SVM regression based on a robust cost function (the  $\varepsilon$ -Huber cost), together with the use of bootstrap resampling techniques for tuning the free parameters of the algorithm [11], [12], can provide us with an efficient HRT denoising technique.

We also propose to study the performance of the denoising procedure in a gold standard given by HRT induced with cardiac electrical stimulation (pacing) during electrophysiological study (EPS), which can be considered an almost noise-free environment, because the patient is maintained at rest. Pacing-induced HRT has started to receive increasing interest, and conditions for its measurement have been established [13], [14], [15], [16], [17]. This gold standard will allow us to quantify the HRT shape in the temporal and spectral domain in an almost noise-free environment, and then to compare the performance of the signal processing algorithms used for HRT denoising in Holter recordings.

The scheme of the paper is as follows. In the next section, the SVM approach to HRT denoising is presented, and other algorithms used for comparison are also described. Then, the algorithms are benchmarked in two scenarios: (1) analysis of induced HRT in a patient database during EPS; and (2) analysis of 24-hour Holter HRT recordings. Finally, conclusions are drawn and future research is suggested.

## II. HRT DENOISING

### A. HRT and PVC Signals

HRT represents a biphasic chronotropic response of sinus rhythm to a single VPC [3], [18], and it is given by an early HR acceleration followed by a deceleration. Its pathophysiological background has been investigated, aiming to understand the underlying mechanisms in order to give an explanation of HRT power as independent postinfarction risk stratifier. It has been hypothesized that HRT could be triggered by a transient vagal inhibition in response to the missed baroreflex afferent input due to hemodynamically inefficient PVC induced ventricular contraction. Late deceleration of HR also increases systolic blood pressure due to vagal recruitment, and hence, this should be consistent with the baroreflex mechanism involved. Physiological mechanisms of HRT and of systolic blood pressure dynamics in the late HRT phase have been studied [18]. HRT could also be influenced by the underlying HR, as far as it defines the hemodynamic setting and the autonomic milieu in which the PVC happens [3].

From a digital signal point of view, HRT signal is a short-length sequence of beat-to-beat time intervals (or R-R intervals), comprising three periods: First, previous 4 or 5 RR intervals represent the basal state in which the PVC occurs; Second, the PVC yields a much shorter interval, followed by a much longer interval due to the compensatory pause; And Third, the turbulence signal consists of the fast initial acceleration, followed by an oscillation in R-R intervals, which usually lasts no longer than about 15-20 beats. Therefore, this is an extremely short signal duration for conventional denoising or filtering techniques.

### B. SVM Denoising Algorithm

According to the preceding description of HRT signal, the signal model considered here uses the NN intervals from an ECG or EGM recording. A PVC has happened at discrete time instant  $n = -1$ , which is then followed by a compensatory pause at  $n = 0$ , so that the following NN intervals (from  $n = 1$  to  $n = 20$ ) represent the PPT under study. Assume that the observed PPT is given by  $\{y_n, n = 1, \dots, 20\}$  contains two contributions: one is the actual HRT as the metabolic response to the PVC perturbation, given by  $\{x_n, n = 1, \dots, 20\}$ , and the other one consists of noise contributions from different sources, and is given by  $\{e_n, n = 1, \dots, 20\}$ . The HRT model is then:

$$y_n = x_n + e_n \quad (1)$$

for  $n = 1, \dots, 20$ . A first approach for denoising  $\{y_n\}$  and obtaining an estimate of HRT, denoted by  $\{\hat{x}_n\}$ , is to use linear filtering. For instance, a  $Q^{th}$  order moving-average filter can be used, which will be given by the following signal model:

$$\hat{x}_n = \sum_{q=1}^Q b_q y_{n-q+1} \quad (2)$$

where  $b_q$  are fixed as the coefficients for an adequate filter in the frequency domain. Independently of the kind of filter used, this denoising scheme relies on the assumption of HRT being a band-limited process. Alternatively, a  $Q^{th}$  median filter can be used, given by

$$\hat{x}_n = \text{median}\{y_{n-\lfloor \frac{Q}{2} \rfloor}, \dots, y_{n+\lceil \frac{Q}{2} \rceil}\} \quad (3)$$

where  $\lfloor \cdot \rfloor$  and  $\lceil \cdot \rceil$  denote the rounding up and down to zero, respectively. This denoising scheme is known to be more appropriated whenever impulse noise can be present.

Note that these basic filtering schemes rely on the distribution of noise being known to some extent, which is an *a priori* information that we do not have yet. According to this fact, we propose to use a SVM modeling approach. The SVM regressor can be seen as a nonparametric procedure, in the sense that it does not rely on any specified form of the HRT. Also, we propose to consider the  $\varepsilon$ -Huber cost [19], which represents a cost function that can adapt itself to the noise distribution. Finally, given that we can not split the extremely short PPT signal into a training and a validation subset, we propose to use nonparametric bootstrap resampling, which has been previously used in SVM classifiers for the same purpose of previously tuning of the SVM free parameters [12].

The SVM model for HRT denoising can be described as follows. The nonlinear regression model is given by

$$y_n = x_n + e_n = \langle \mathbf{w}, \phi(n) \rangle + b + e_n \quad (4)$$

where  $\phi(n)$  is a nonlinear application of  $n$  to a possibly high-dimensional (say  $P$ -dimensional) feature space  $\mathfrak{F}$ , where a linear approximation is built by the dot product with vector  $\mathbf{w} \in \mathfrak{F}$ . This model can be seen as a nonlinear interpolation. Following the conventional SVM methodology, a regularized cost function of the residuals is to be minimized. In [19], the following robust cost function of the residuals was proposed,

$$L(e_n) = \begin{cases} 0, & |e_n| \leq \varepsilon \\ \frac{1}{2\delta}(|e_n| - \varepsilon)^2, & \varepsilon \leq |e_n| \leq e_C \\ C(|e_n| - \varepsilon) - \frac{1}{2}\delta C^2, & |e_n| \geq e_C \end{cases} \quad (5)$$

where  $e_C = \varepsilon + \delta C$ ;  $\varepsilon$  is the insensitive parameter, and  $\delta$  and  $C$  control the trade-off between the regularization and the losses. The  $\varepsilon$ -insensitive zone ignores errors lower than  $\varepsilon$ ; the quadratic cost zone uses the  $L_2$ -norm of errors, which is appropriate for Gaussian noise; and the linear cost zone controls the effect of outliers. The SVM coefficients are estimated by minimizing the previous loss function regularized with the squared norm of model coefficients,

$$\frac{1}{2} \sum_{p=1}^P w_p^2 + \frac{1}{2\delta} \sum_{n \in I_1} (\xi_n^2 + \xi_n^{*2}) + C \sum_{n \in I_2} (\xi_n + \xi_n^*) - \sum_{n \in I_2} \frac{\delta C^2}{2} \quad (6)$$

with respect to  $w_p$ ,  $\{\xi_n^{(*)}\}$  (notation for both  $\{\xi_n\}$  and  $\{\xi_n^*\}$ ), and  $b$ , and constrained to

$$y_n - \langle \mathbf{w}, \phi(n) \rangle - b \leq \varepsilon + \xi_n \quad (7)$$

$$-y_n + \langle \mathbf{w}, \phi(n) \rangle + b \leq \varepsilon + \xi_n^* \quad (8)$$

$$\xi_n, \xi_n^* \geq 0 \quad (9)$$

for  $n = 1, \dots, 20$ ;  $\{\xi_n^{(*)}\}$  are *slack variables* or *losses*, which are introduced to handle the residuals according to the robust cost function; and  $I_1, I_2$  are the sets of samples for which losses have a quadratic or a linear cost, respectively.

Similar derivations of the dual functional can be found in the literature [19], [20]. In brief, by including linear constraints (7)-(9) into (6), the primal-dual functional (or Lagrange functional) is obtained:

$$\begin{aligned} L_{PD} = & \frac{1}{2} \sum_{p=1}^P w_p^2 + \frac{1}{2\delta} \sum_{n \in I_1} (\xi_n^2 + \xi_n^{*2}) + C \sum_{n \in I_2} (\xi_n + \xi_n^*) - \\ & - \sum_{n \in I_2} \frac{\delta C^2}{2} - \sum_{n=1}^{20} (\beta_n \xi_n + \beta_n^* \xi_n^*) - \varepsilon \sum_{n=1}^{20} (\alpha_n + \alpha_n^*) + \\ & + \sum_{n=1}^{20} (\alpha_n - \alpha_n^*) (y_n - \langle \mathbf{w}, \phi(n) \rangle - b - \xi_n) \end{aligned} \quad (10)$$

constrained to  $\alpha_n^{(*)}, \beta_n^{(*)}, \xi_n^{(*)} \geq 0$ . By making zero the gradient of  $L_{PD}$  with respect to the primal variables [19], we obtain  $\alpha_n^{(*)} = \frac{1}{\delta} \xi_n^{(*)}$  ( $n \in I_1$ ),  $\alpha_n^{(*)} = C - \beta_n^{(*)}$  ( $n \in I_2$ ), to be fulfilled, and if these constraints are included into (10), primal variables can be removed. The correlation matrix of input space vectors

can be identified, and denoted as  $\mathbf{R}(s, t) \equiv \langle \phi(s), \phi(t) \rangle$ . The dual problem can now be obtained and expressed in matrix form, and it corresponds to the maximization of

$$-\frac{1}{2} (\boldsymbol{\alpha} - \boldsymbol{\alpha}^*)^T [\mathbf{R} + \delta \mathbf{I}] (\boldsymbol{\alpha} - \boldsymbol{\alpha}^*) + (\boldsymbol{\alpha} - \boldsymbol{\alpha}^*)^T \mathbf{y} - \varepsilon \mathbf{1}^T (\boldsymbol{\alpha} + \boldsymbol{\alpha}^*) \quad (11)$$

constrained to  $C \geq \alpha_n^{(*)} \geq 0$ , where  $\boldsymbol{\alpha}^{(*)} = [\alpha_1^{(*)}, \dots, \alpha_{20}^{(*)}]^T$ ;  $\mathbf{y} = [y_1, y_2, \dots, y_{20}]^T$ ; and  $\mathbf{1}$  denotes a column vector of ones. After obtaining Lagrange multipliers  $\boldsymbol{\alpha}^{(*)}$ , the time series model for a sample at time instant  $m$  is:

$$\hat{x}_m = \sum_{n=1}^{20} (\alpha_n - \alpha_n^*) \langle \phi(n), \phi(m) \rangle + b \quad (12)$$

which is a weighted function of the nonlinearly observed times in the feature space. Note that only a reduced subset of the Lagrange multipliers is nonzero, which are called the *support vectors*, and the HRT solution is built in terms of them.

A Mercer's kernel is a bivariate function that is equivalent to calculate a dot product in a possibly infinite dimensional feature space [10]. Examples of valid Mercer's kernels are the *linear kernel*, given by  $K(s, t) = \langle s, t \rangle$ , and the (nonlinear) *Gaussian kernel*, given by

$$K_G(s, t) = \exp\left(-\frac{(s-t)^2}{2\sigma^2}\right) \quad (13)$$

where  $\sigma$  is the width of the Gaussian kernel, and it must be properly chosen. For a fixed value of  $\sigma$ , it is fulfilled that  $K_G(s, t) = \langle \phi(s), \phi(t) \rangle$  in some unknown feature space. However, we do not need to know explicitly neither the feature space nor the nonlinear application, but still the dot products in the feature space can be readily calculated by means of the kernel. Thus, the final solution of SVM for HRT denoising can be expressed simply as

$$\hat{x}_m = \sum_{n=1}^{20} (\alpha_n - \alpha_n^*) K_G(n, m) + b \quad (14)$$

which is just a linear combination of shifted Gaussian kernels of a given width.

### C. Bootstrap Tuning of the Free Parameters

Note that several free parameters need to be previously tuned in the described SVM denoising algorithm, namely, width  $\sigma$  of the Gaussian kernel, and the free parameters of the cost function ( $\varepsilon, \delta, C$ ). Cross-validation techniques are often used for this purpose in SVM approaches, but in our case only 20 observations are available, and splitting them involves dramatically reducing the amount of information in the training set. We propose to search using bootstrap resampling techniques for finding the bootstrap bias-corrected error as a function of each free parameter, and then fixing the free parameters and training a machine with the whole 20-samples set of the PPT.

Bootstrap resampling techniques are useful for nonparametric estimation of the *pdf* of statistical magnitudes, even when the observation set is small. A detailed description and discussion on bootstrap resampling can be found in [21]. The

procedure used here is described in [12] for SVM classification, its extension to the regression case being straightforward. In brief, be  $\theta = \{\varepsilon, \delta, C\}$  is the set of free parameters of the SVM for time series  $y_n$ . The estimated SVM coefficients are  $\hat{\alpha} = [\hat{\alpha}_1 - \hat{\alpha}_1^*, \dots, \hat{\alpha}_{20} - \hat{\alpha}_{20}^*] = s(\{y_n\}, \theta)$ , where  $s(\cdot)$  denotes the SVM estimation operator. Empirical risk  $\hat{R}_{emp} = t(\hat{\alpha}, \{y_n\})$ , where  $t(\cdot)$  is the estimation operator, can be defined as the averaged cost in the training set of samples. A *bootstrap resample* is a data subset drawn from the training set by following its empirical distribution, and accordingly, it consists of sampling with replacement the time samples of  $y_n$ , this is,  $\{y_n^*(b)\} = \{y_1^*, y_2^*, \dots, y_{20}^*\}$ , and the resampling process is repeated for  $b = 1, \dots, B$  times. Note that, for each resample,  $\{y_n^*(b)\}$  contains samples of  $\{y_n\}$  appearing none, one, or several times. A partition of  $\{y_n\}$  set of samples can be done in terms of resample  $y_n^*(b)$ , given by  $\{y_n\} = \{y_{n,in}^*(b)\} \cup \{y_{n,out}^*(b)\}$ , according to the time samples included (in) and excluded (out) in resample  $b$ . The SVM coefficients from each resample will be given by  $\hat{\alpha}(b) = s(\{y_1, \dots, y_{n,in}^*(b)\}, \theta)$ .

An acceptable approximation to the actual risk (i.e., not only empirical, but total risk) can be obtained if we use  $\hat{R}_{act} = t(\hat{\alpha}(b), \{y_{n,out}^*(b)\})$ . A bias-corrected estimate of the actual risk is obtained by simply taking the replication average. Furthermore, this average estimate can be achieved for a grid of values of the SVM free parameters, hence allowing us to determine their suitable values to train the SVM with the whole training set. A good range for B is typically 200 to 500 resamples. SVM free parameters are not usually mutually independent, however, a good heuristic approach is to start with an intermediate value of  $C, \gamma$ , set  $\varepsilon = 0$ , then giving an initial guess of the kernel parameter, and then re-estimate again each the other parameters, continuing until a stable set of parameters is obtained.

### III. EXPERIMENTS

Practical issues for the application of the proposed HRT denoising techniques were studied and are next presented. We start by analyzing the suitability of bootstrap resampling for tuning the free parameters in SVM interpolation algorithm. Then, the clinical EPS database that was used as gold standard for HRT measurements is described, and application examples of denoising are used in order to show the following points: (1) pacing-induced HRT during EPS can be considered as almost noise-free recordings; (2) The cycle length previous to the HRT onset can be physiologically related to the HRT oscillation amplitude, which should be taken into account when measuring TS parameter; And (3) the spectral domain representation of HRT can yield the shape of the denoised gold standard HRT. Next, measurements on TS parameter are studied in the gold standard EPS patient database. After summarizing the clinical data of Holter database, denoising examples are considered both in the time and in the frequency domains, and plobational measurements of TS are studied in this setting. Finally, denoising methods are statistically compared in terms of a new parameter, the Turbulence Length, which allows us to quantitatively determine the effectiveness of the denoising procedures in the time domain.

#### A. SVM Free Parameter Selection

One of the key issues when using SVM algorithms is setting appropriate values for the free parameters. In this problem, where only 20 discrete-time samples are available, bootstrap resampling was used for this purpose. For each PPT, the Mean Squared Error (MSE) was estimated with Bootstrap resampling on the time series for each tested combination of SVM free parameters ( $C, \gamma, \varepsilon$ , and  $\sigma$ ). Bootstrapped MSE (200 resamplings) was obtained for values of each free parameter in its search interval, while freezing the other parameters, using a sequential search and with two rounds. Figure 1(a) shows an example of the bootstrapped MSE for searching the free parameters in a PPT of a patient, and panel (b) depicts the histograms of the free parameters obtained for all the PPT in the same patient. An appropriate rank of searched values was set by reviewing the histograms in a subset of the EPS and Holter database, which was found to be  $\gamma \in (10^{-3}, 0.32)$ ,  $C \in (1, 600)$  and  $\sigma \in (1.5, 6)$  (on a logarithmic scale), and  $\varepsilon$  between 0 and the standard deviation of the signal divided by 10 (on a linear scale). These ranks were found to be appropriate for individually tuning in each PPT the SVM interpolator throughout the study.

#### B. EPS Patient Data Set

PPTs were induced by pacing in 10 patients with structurally normal heart during EPS under mild sedation at rest and were used as the HRT gold standard by assuming that under these conditions the electrophysiological noise would be minimized. The PVCs were induced by cyclic pacing from the right ventricular apex, after every twenty one spontaneous beats during sinus rhythm, according to the procedure suggested in [16]. The intracardiac EGM and the surface ECG were simultaneously recorded on a conventional digital polygraph and the beat-to-beat intervals were extracted from the ECG.

Figure 2 shows an example of denoising a PPT in a patient from EPS database. A clear smoothing effect can be observed, and the turbulence oscillation pattern (this is, initial acceleration followed by a deceleration) is clearly recovered with the three methods, i.e., SVM, linear (FIR), and median (MED) filtering. According to its proposal as gold standard, low noise level is expected in these signals, and hence, they hardly differ from the denoised version with any of the proposed algorithms. This can be also checked in the frequency domain representation of the HRT. We obtained the spectrum using a Fast Fourier Transform (FFT) of 512 samples for the PPT recording. Note the extremely low length of the HRT time series (20 samples), which makes a strong windowing effect to be present. Figure 2 also shows the power spectral density for denoised PPTs. It can be seen that the power in low frequency (about  $< 0.18$  Hz) is maintained in all cases, whereas the high frequency components are filtered and smoothed, aiming to cancel the high frequency noise. The SVM denoised signal has a slightly lower level in the high frequency band (about  $> 0.18$  Hz) and a less distorted low frequency band, when compared to the spectrum of the other denoising methods.

The relationship with previous cycle length was observed in the gold standard HRT. Figure 3 shows an example of the

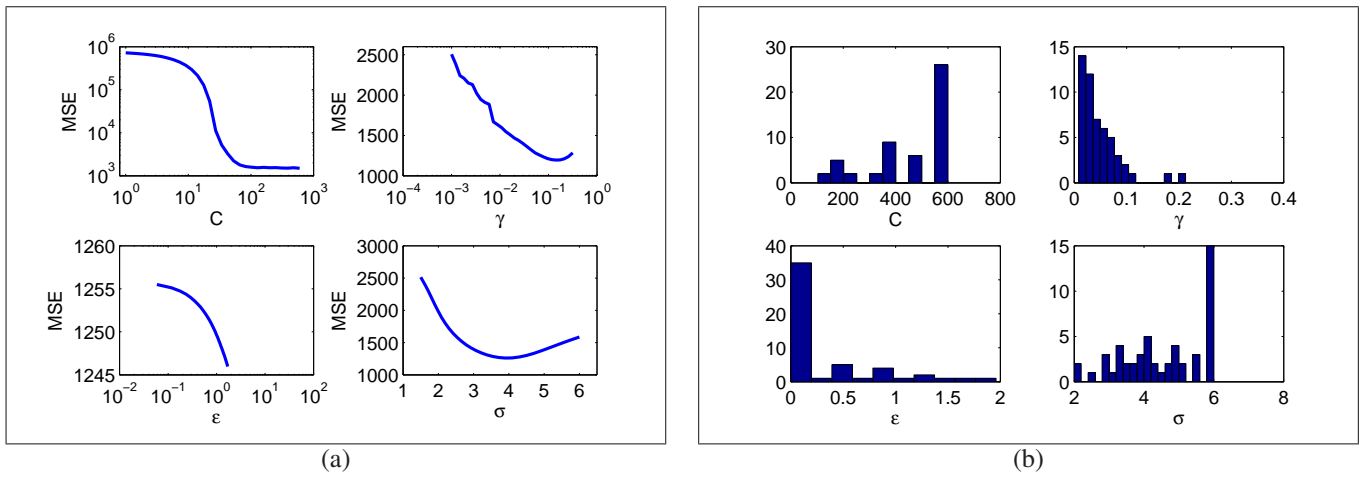


Fig. 1. Example of free parameters selection for the SVM denoising algorithm. (a) Bootstrap estimated MSE in a single PPT example. Each free parameter is subsequently explored in a rank of possible values while fixing the other ones. (b) Histograms of the obtained values of the free parameters for a set of PPT in a single patient. Note the trend of  $\gamma$  and  $\epsilon$  towards lower values, and of  $C$  and  $\sigma$  towards higher values.

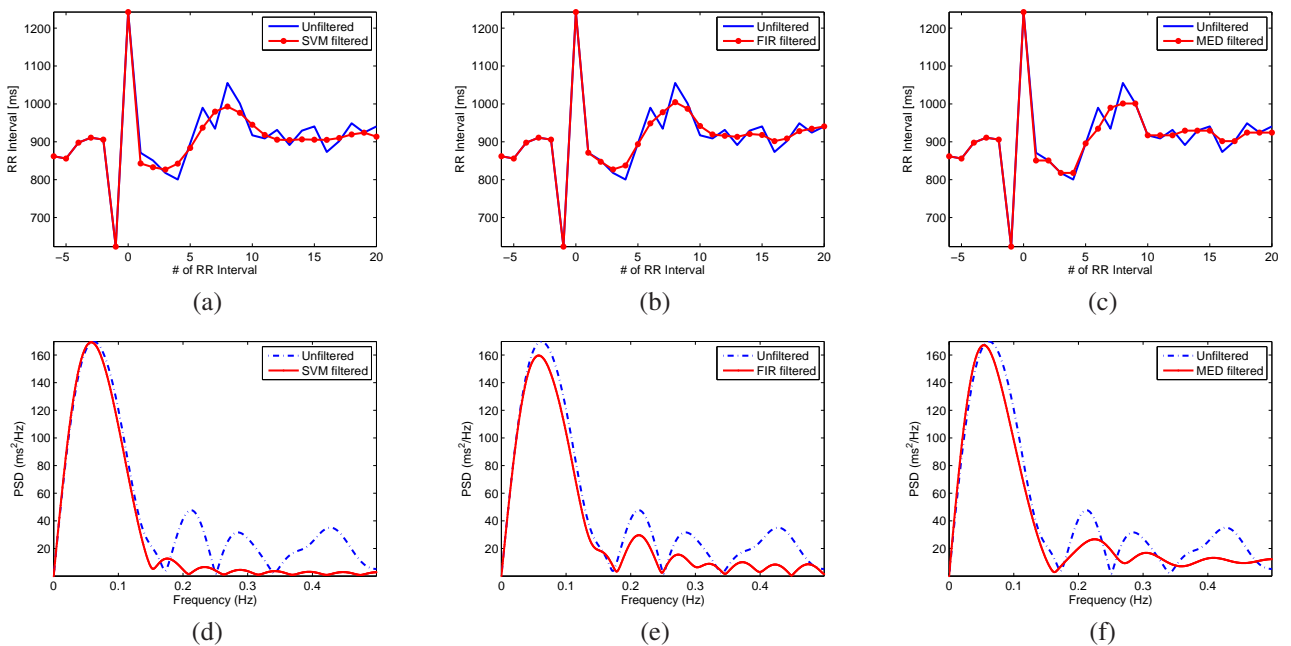


Fig. 2. EPS database: Examples of HRT denoising, in time (left) and frequency (right) domains. (a,d) SVM filtered. (b,e) FIR filtered. (c,f) Median filtered.

effect of the preceding cycle in a patient with three different conditions: basal, low, and high doses of isoproterenol, yielding different levels of HR acceleration preceding the HRT. In order to clearly observe the relationship between the HR and the HRT, a number between 9 and 11 PVC were stimulated for each of these states. Figure 3(a) shows the relationship between preceding HR and HRT oscillation amplitude in the time domain. According to previously reported results in the literature [3], the increase in HR is related to a decrease in the turbulence oscillation amplitude. Figure 3(b) shows the same effect in the frequency domain, in which the spectral envelope clearly decreases with cycle length. Note also that there is a slight, yet visible, shift in the power towards lower bands. Figure 3(c) shows the normalized spectra, in which the shift is still more patent. Accordingly, filtering the averaged PPT, while being adequate for noise reduction, may mask

the potential changes of the PPT response over time, thus precluding to assess oscillations of the autonomic balance in an individual patient. Figure 3(d) shows the averaged spectrum and 95% confidence intervals for normalized spectrum in a patient of EPS database, for raw and denoised signals. Spectra of each PPT have been separately normalized, and average and standard deviation have been subsequently calculated.

Note that filtering does not change significantly the spectral content of the turbulence in physiological rest with any of the denoising methods, which allows us to consider pacing induced HRT during EPS as a gold standard for comparison with the denoising algorithms in the Holter database.

### C. Results on the EPS Patient Data Set

Table I shows the number of PVC (PPT) obtained for each patient in the EPS database, together with the mean and

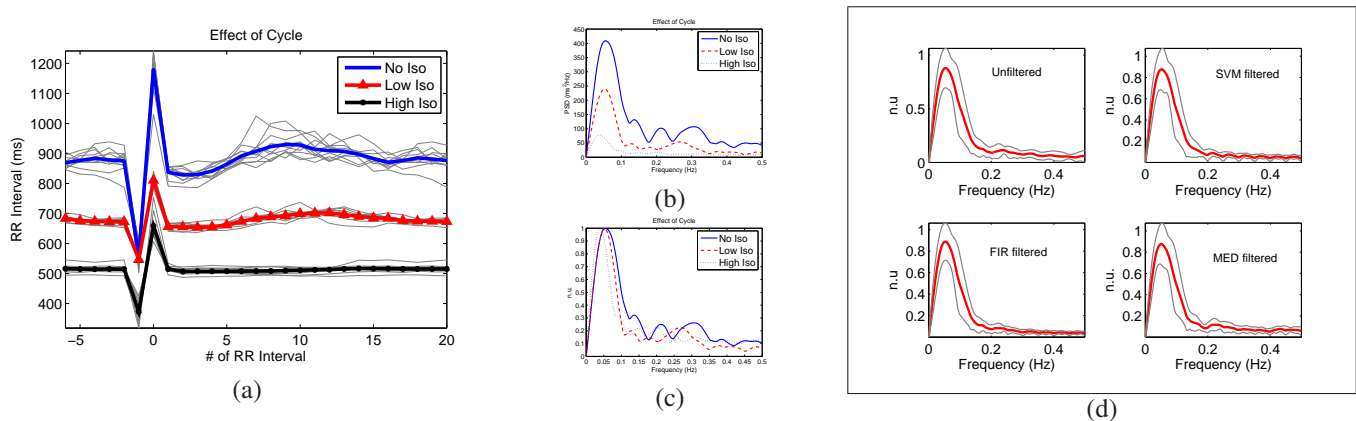


Fig. 3. EPS database: Relationship with preceding cycle length. (a) PPTs for basal and for low and high isoproterenol dosing controlling the heart rate. (b) Effect of cycle in frequency domain. (c) Effect of cycle in frequency domain, with normalized units. (d) Normalized spectra for a patient (mean and 95% CI), for raw and denoised PPT.

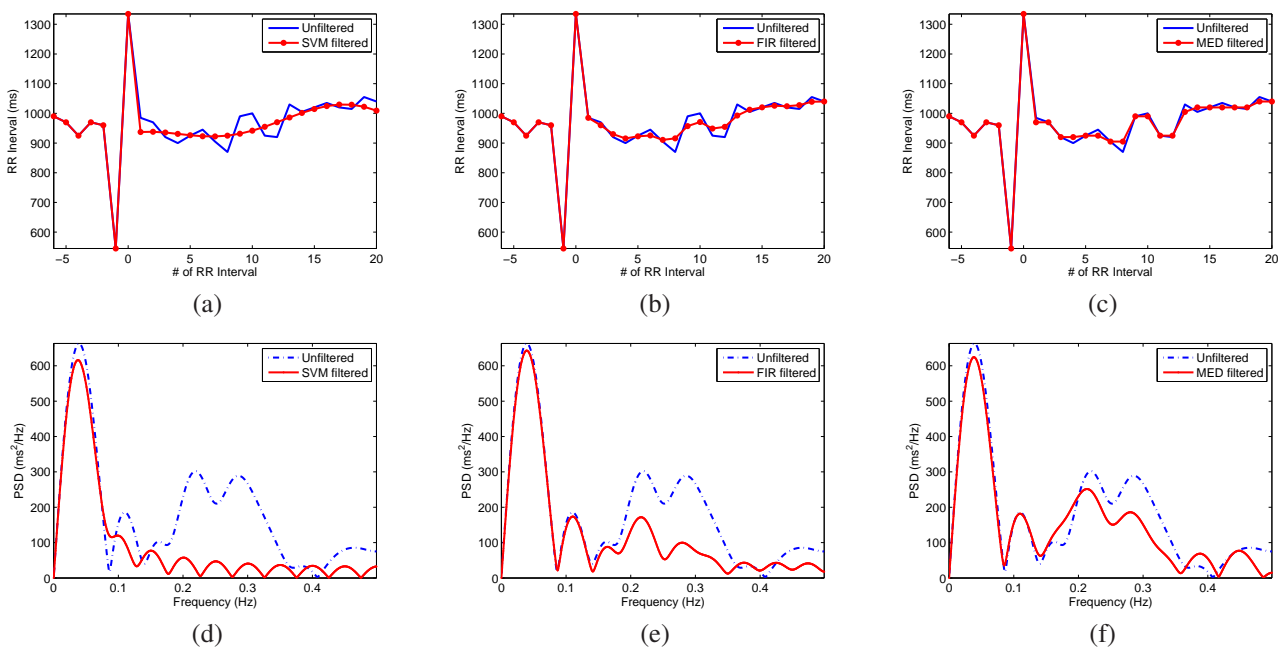


Fig. 4. Examples in Holter database, in time (up) and frequency (down) domains: (a,d) SVM denoised; (b,e) FIR denoised; (c,f) Median denoised.

standard deviation of the  $TS$  parameter in each PPT ( $TS_{PPT}$ ), both for unfiltered and for filtered conditions. Right columns in the table present the values of the  $TS$  parameter for each patient, and for each denoising algorithm ( $SVM\ TS$ ,  $FIR\ TS$ ,  $Median\ TS$ ), as well as for the raw signal. Parameter  $TS$  was here obtained according to the conventional procedure, i.e., by calculating the  $TS$  for the averaged PPT signals. It can be seen that parameter  $TS$  has lower values when obtained from the averaged template than when averaged in each PPT. Nevertheless, in both cases the  $TS$  has similar values (yet slightly lower for the denoised PPTs) for all the denoising methods.

#### D. Holter Data Set

PPTs were also obtained in 61 post-myocardial infarction patients included in a prospective study at a tertiary University Hospital [22]. A 24-hour ambulatory electrocardiographic

monitoring was performed in patients with stable sinus rhythm between 2 and 6 weeks after infarction and 61 with at least 1 PVC during the monitoring period were included in the analysis (age  $64.3 \pm 9.0$  years, 26 men). The average number of PPTs per patient was 50.7 (median 12, rank 1-474).

Figure 4 shows a denoising example in one of these patients. It can be seen that SVM obtains a denoised signal with a clearer turbulence pattern in the time domain in comparison with the other two filtering methods. With respect to the frequency domain, SVM is better than the other denoising methods at canceling the noisy components in high frequency, while preserving an spectral shape that is quite similar to the previously observed in the gold standard. Averaged normalized spectra and 95% confidence intervals with all the methods are shown in Figure 5, in two patients with moderate and low (24 and 8) number of PPTs in the 24-hour recording. The unfiltered spectra show an extremely high noise level that is

# Pat	# PVC	$TS_{PPT}$	SVM $TS_{PPT}$	FIR $TS_{PPT}$	Median $TS_{PPT}$	TS	SVM TS	FIR TS	Median TS
Pat1	9	34.7 ± 10.9	33.2 ± 11.9	28.6 ± 9.7	30.3 ± 12.8	30.2	29.5	25.3	28.1
Pat2	11	24.6 ± 7.8	22.7 ± 7.1	21.9 ± 7.3	23.6 ± 7.9	19.7	18.4	18.6	20.1
Pat3	10	61.1 ± 27.9	51.2 ± 26.7	46.4 ± 22.3	48.7 ± 26.8	52.7	41.7	40.2	40.0
Pat4	9	38.7 ± 27.7	30.8 ± 24.2	30.3 ± 22.4	29.4 ± 21.2	17.6	15.0	14.0	15.5
Pat5	11	47.0 ± 13.3	33.5 ± 10.6	36.5 ± 9.4	37.3 ± 10.6	41.6	30.9	35.2	35.2
Pat6	8	13.0 ± 4.2	10.2 ± 5.1	9.9 ± 3.5	10.9 ± 4.8	7.8	6.6	6.6	6.6
Pat7	11	24.6 ± 10.1	19.0 ± 7.2	20.7 ± 8.0	22.0 ± 9.0	20.6	16.8	18.9	19.8
Pat8	12	24.1 ± 15.5	18.5 ± 14.1	19.5 ± 14.2	21.3 ± 16.7	14.3	11.0	12.2	13.9
Pat9	14	33.8 ± 15.2	28.8 ± 11.3	28.8 ± 12.3	31.0 ± 13.1	28.0	24.4	24.4	25.6
Pat10	19	8.6 ± 2.9	7.6 ± 3.0	7.4 ± 2.7	7.9 ± 3.1	6.3	5.9	5.7	6.0

TABLE I

EPS DATABASE RESULTS: NUMBER OF PVC PER PATIENT,  $TS$  PARAMETER FOR EACH PATIENT AND EACH PPT (MEAN ± STANDARD DEVIATION), AND  $TS$  PARAMETER FROM AVERAGED PPT ( $TS_{PPT}$ ) AFTER DENOISING.

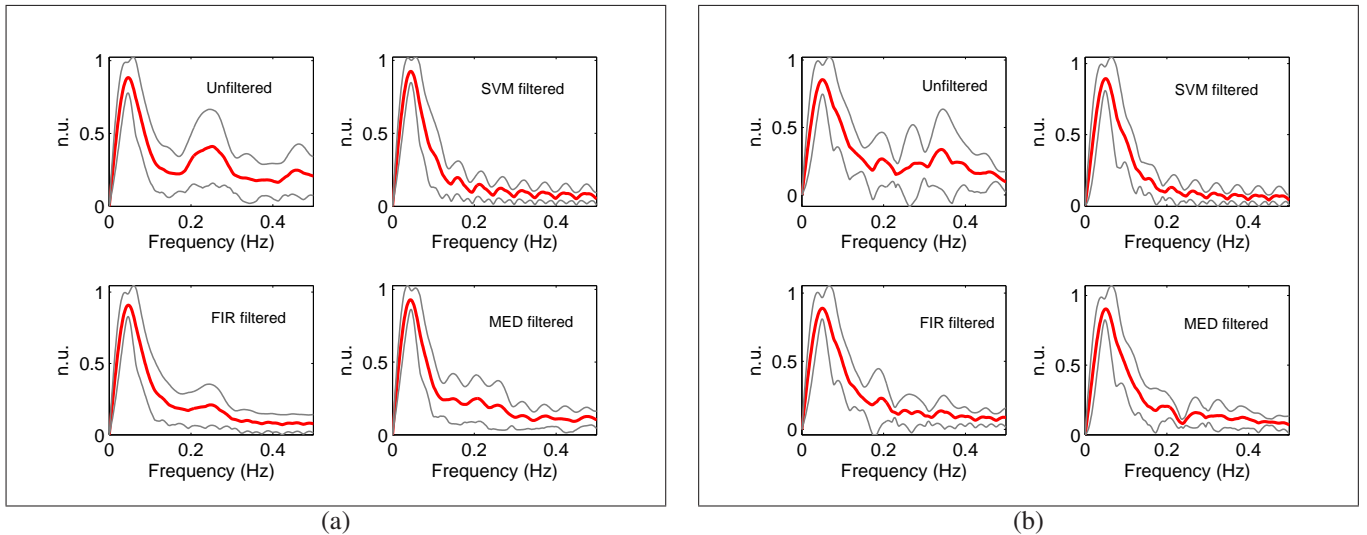


Fig. 5. Examples from Holter database in the frequency domain. Averaged normalized spectra and 95% confidence intervals for two patients with 24 PPT (a) and 8 PPT (b) in their 24-hours Holter recordings.

partially reduced by the median and FIR algorithms. However, the narrower confidence interval and shape coherence with the gold standard spectra is obtained with the SVM denoising.

### E. Results on the Holter Data Set

Table II shows the number of PPTs in the Holter database. Also, the values of  $TS$  parameter when obtained from conventional processing for both raw and denoised signals were compared with its calculation from each isolated PPT ( $TS_{PPT}$ ) in all cases. As expected, higher  $TS$  values were obtained for isolated and denoised PPT, and in both procedures, SVM denoised values yielded the lowest standard deviation.

An additional parameter was calculated, aiming to quantify the similarity in the time domain between the (raw or denoised) actual PPT and the expected according to the physiological definition of HRT. Therefore, for each PPT we obtained the following sequence: first minimum, first maximum, and second minimum, for the raw and for the filtered PPT. This sequence gives a measurement of the similarity between the turbulence waveform and the postulated mechanism in the HRT definition (deceleration, acceleration, and oscillation). The Turbulence Length parameter was calculated as the difference between the discrete times corresponding to the second and to the first minimum, and hence it has units of number of beats.

	Mean±Std	Median	[Max,Min]
# PPT	50.7 ± 104.8	12	[474, 1]
TS	7.8 ± 6.0	6.1	[29.1, 0.4]
SVM TS	6.9 ± 4.4	6.1	[20.3, 0.4]
FIR TS	6.8 ± 6.3	5.2	[37.3, 0.2]
Median TS	6.8 ± 6.3	5.2	[37.3, 0.2]
$TS_{PPT}$	14.7 ± 9.8	12.1	[174.0, 0]
SVM $TS_{PPT}$	11.3 ± 6.0	10.6	[145.4, 0.02]
FIR $TS_{PPT}$	11.9 ± 8.3	9.6	[146.1, 0.002]
Median $TS_{PPT}$	13.2 ± 10.0	10.7	[171.5, 0]

TABLE II  
HOLTER DATABASE: NUMBER OF PPT PER PATIENT AND VALUES FOR THE  $TS$  PARAMETER (RAW AND DENOISED). CONVENTIONALLY CALCULATED AND AVERAGED VALUES FOR INDIVIDUAL TS FROM DENOISED HRT ( $TS_{PPT}$ ) ARE REPORTED.

	Tach.	SVM	FIR	Med.
EPS	5.2±1.7	10.9±3.0*	9.7±2.5*	7.2±2.4*
Holter	3.0±0.7	11.2±2.6*	7.6±2.7*	5.3±1.6*

TABLE III  
EPS AND HOLTER DATABASES: TURBULENCE LENGTHS FOR THE PATIENTS IN THE STUDY AND FOR THE DENOISING ALGORITHMS.

Figure 6 shows an example in a patient with a high number of PPT, and it can be observed therein that the Turbulence

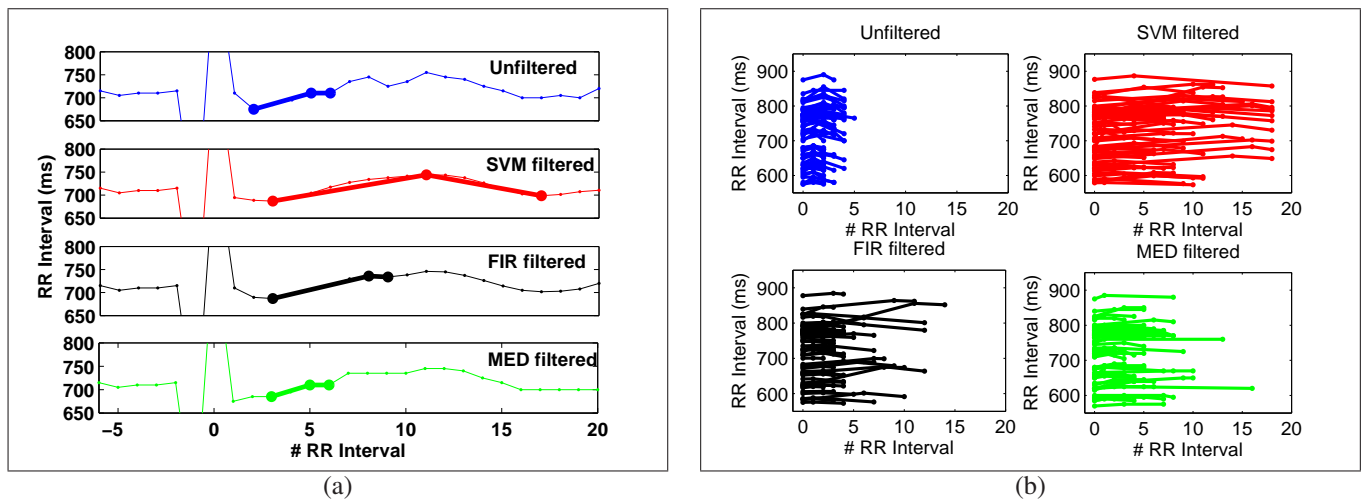


Fig. 6. Holter Database: Examples of Turbulence Length calculation. (a) When Turbulence Length is measured in a single PPT, larger values correspond to a clearer correspondence with the oscillation expected by the HRT mechanism, whereas shorter values are in general due to noise still present in the signal. (b) Example of Turbulence Lengths in a patient with high number of PPT, and effect of the denoising algorithms.

Length is extremely short in raw PPT, because the first and second relative minima usually correspond to the noise present in the signal. An increase in the turbulence length can be obtained for denoising PPT, which is more visible with the SVM denoising. Table III shows the values of the Turbulence Length both in the gold standard and in the Holter databases, in which a significant increase can be observed ( $*p < 0.001$  when compared with unfiltered tachograms, paired t-Student test).

#### IV. CONCLUSIONS

A new signal processing method, the SVM interpolation, has been proposed for denoising PPT signals in HRT. The use of a gold standard database with pacing induced PPT during EPS has been used for comparison of the HRT behavior both in the time and in the spectral domains. In low-noise conditions, the SVM algorithm yielded results that were similar to other conventional filtering methods, and in all cases the results were according to the expected mechanism of the HRT. For PPTs in this EPS database, denoising algorithms also were shown to yield similar spectral profiles of HRT. In the presence of noise, i.e., in the Holter database, the tested algorithms yielded denoised PPT signals containing lower noise level. However, SVM algorithm obtained a higher performance when compared to the median and to the FIR filters. As seen in the examples, the oscillations that are expected in the HRT were better preserved, the spectral profile of the denoised PPT was more similar to the observed in the gold standard, standard deviation was lower, and the significantly higher values of Turbulence Length suggest that the noise was more efficiently removed from the turbulence.

The proposed SVM algorithm allows to perform the HRT analysis even when a low number of PVCs are available. This characteristic has clinical implications, because one of the current requirements for suitability of a patient to be studied in terms of  $TS$  is a sufficient number of PVCs being available. Thus, HRT denoising will help to extend the HRT analysis to a higher number of patients. The SVM algorithm gives a better description of the dependence with the HR previous

to the PPT, and allows the analysis of the changes of HRT with time. These possibilities should be explored in additional studies with other databases of patients with different cardiac diseases.

We can conclude that it is possible to obtain time-local HRT measurements without averaging, by using robust digital signal processing, as shown by the analysis on the EPS database. The SVM denoising allows us to measure the HRT in noisy conditions, such as in patients with Holter, which is a usual situation in the clinical practice. Finally, this denoising can give new approaches to HRT analysis, such as evaluation of the changes of HRT with time, or the evaluation of patients with a low number of PVC. Hence, the application of SVM denoising in series with clinical events could improve the predictive value of the classical HRT methods for risk stratification. Finally, other similar problems can be found in Electroencephalography literature, like event-related potentials [23], [24], which could be addressed by following the approach used here to HRT denoising.

#### REFERENCES

- [1] G. Schmidt, M. Malik, P. Barthel, R. Schneider, K. Ulm, L. Rolnitzky, A. J. Camm, J. T. Bigger Jr, and A. Schömig, "Heart-rate turbulence after ventricular premature beats as predictor of mortality after acute myocardial infarction," *Lancet*, vol. 353, pp. 1390–1396, 1999.
- [2] M. Watanabe and G. Schmidt, "Heart rate turbulence: A 5-year review," *Heart Rhythm*, vol. 1, pp. 732–738, 2004.
- [3] A. Bauer, M. Malik, P. Barthel, R. Schneider, M. A. Watanabe, A. J. Camm, A. Schomig, and G. Schmidt, "Turbulence dynamics: An independent predictor of late mortality after acute myocardial infarction," *International Journal of Cardiology*, no. 107, pp. 42–7, 2005.
- [4] F. Tundo, F. Lombardi, M. C. Rocha, F. Botoni, G. Schmidt, V. C. Barros, B. Muzzi, M. Gomes, A. Pinto, and A. L. Ribeiro, "Heart rate turbulence and left ventricular ejection fraction in chagas disease," *Europace*, vol. 7, pp. 197–203, 2005.
- [5] J. Koyama, J. Watanabe, A. Yamada, Y. Koseki, Y. Konno, S. Toda, T. Shinozaki, M. Miura, M. Fukuchi, M. Ninomiya, Y. Kagaya, and K. Shirato, "Evaluation of heart-rate turbulence as a new prognostic marker in patients with chronic heart failure," *Circ J*, vol. 66, pp. 902–907, 2002.
- [6] A. P. Hallstrom, P. K. Stein, R. Schneider, M. Hodges, G. Schmidt, and K. Ulm, "Characteristics of heart beat intervals and prediction of death," *International Journal of Cardiology*, vol. 100, pp. 37–45, 2005.



- [7] J. Schwab, G. Eichner, G. Veit, H. Schmitt, T. Lewalter, and B. Luderitz, "Influence of basic heart rate and sex on heart rate turbulence in healthy subjects," *PACE*, vol. 27, pp. 1625–1631, 2004.
- [8] A. P. Hallstrom, P. K. Stein, R. Schneider, M. Hodges, G. Schmidt, and K. Ulm, "Structural relationships between measures based on heart beat intervals: Potential for improved risk assessment," *IEEE Trans Biomed Eng*, vol. 51, pp. 1414–20, 2004.
- [9] I. Cygankiewicz, J. Wranciz, H. Bolinska, J. Zaslonka, and W. Zareba, "Circadian changes in heart rate turbulence parameters," *J Electrocardiol*, vol. 37, no. 4, pp. 297–303, 2004.
- [10] V. Vapnik, *The Nature of Statistical Learning Theory*. New York: Springer-Verlag, 1995.
- [11] J. L. Rojo-Álvarez, G. Camps-Valls, M. Martínez-Ramón, E. Soria-Olivas, A. Navia Vázquez, and A. R. Figueiras-Vidal, "Support vector machines framework for linear signal processing," *Sig Proc*, vol. 85, no. 12, pp. 2316–26, 2005.
- [12] J. L. Rojo-Álvarez, A. Arenal-Maíz, and A. Artés-Rodríguez, "Discriminating between supraventricular and ventricular tachycardias from EGM onset analysis," *IEEE Eng Med Biol*, vol. 21, pp. 16–26, 2002.
- [13] N. Guettler, D. Vukajlovic, A. Berkowitsch, B. Schulte, A. Erdogan, J. Carlsson, J. Neuzner, and H. Pitschner, "Effect of vagus blockade with atropine on heart rate turbulence," *PACE*, vol. 24 Part II, p. 625, 2001.
- [14] I. Savelieva, D. Wichterle, M. Harries, M. Meara, J. Camm, and M. Malik, "Different effects of atrial and ventricular prematurity on heart rate turbulence: relation to left ventricular function," *PACE*, vol. 25 Part II, p. 608, 2002.
- [15] M. Watanabe and M. Josephson, "Heart rate turbulence in the spontaneous ventricular tachy-arrhythmia database," *PACE*, vol. 23, no. Part II, p. 686, 2000.
- [16] M. Watanabe, J. Marine, M. Sheldon, and M. Josephson, "Effects of ventricular premature stimulus coupling interval on blood pressure and heart rate turbulence," *Circulation*, vol. 106, pp. 325–330, 2002.
- [17] D. Roach and R. Sheldon, "Turbulence: a focal, inducible, source of heart period variability associated with induced, transient hypertension," *PACE*, vol. 23, no. Part II, p. 709, 2000.
- [18] D. Wicherle, V. Melenovsky, J. Simek, J. Malik, and M. Malik, "Hemodynamics and autonomic control of heart rate turbulence," *J Cardiovasc Electrophysiol*, vol. 17, pp. 286–91, 2006.
- [19] J. L. Rojo-Álvarez, M. Martínez-Ramón, A. R. Figueiras-Vidal, M. de Prado Cumplido, and A. Artés-Rodríguez, "Support vector method for ARMA system identification," *IEEE Trans Sig Proc*, vol. 52, no. 1, pp. 155–64, 2004.
- [20] G. Camps-Valls, J. L. Rojo-Álvarez, and M. Martínez-Ramón, *Kernel Methods in Bioengineering, Signal and Image Processing*. Hershey, PA (USA): Idea Group Inc., 2006.
- [21] B. Efron and R. Tibshirani, *An Introduction to the Bootstrap*. Chapman&Hall, 1998, vol. 57.
- [22] J. González-Carrillo, A. García-Alberola, D. Saura, P. Carrillo, R. López, J. J. Sánchez-Muñoz, J. Martínez, and M. Valdés, "Impacto de la angioplastia primaria en la indicación de desfibrilador implantable en pacientes con infarto de miocardio," *Rev Esp Cardiol*, vol. 56, no. 12, pp. 52–56, 2003.
- [23] P. Jaskowski and R. Verleger, "Amplitudes and Latencies of Single trial ERP's Estimated by a Maximum-likelihood Method," *IEEE Trans Biomed Eng*, vol. 46, pp. 987–93, 1999.
- [24] D. Lange, H. Siegelmann, H. Pratt, and G. Inbar, "Overcoming selective averaging: Unsupervised identification of event-related brain potentials," *IEEE Tran Biomed Eng*, vol. 47, pp. 822–26, 2000.



**José Luis Rojo-Álvarez (Member, 01)** received the Telecommunication Engineering Degree in 1996 from University of Vigo, Spain, and the PhD in Telecommunication in 2000 from the Polytechnical University of Madrid, Spain. Since 2006, he has been an Associate Professor in the Department of Signal Theory and Communications, University Rey Juan Carlos, Madrid, Spain. He has published more than 30 papers and more than 70 international conference communications. His main research interests

include statistical learning theory, digital signal processing, and complex system modeling, with applications to digital communications and to cardiac signal and image processing.



**Óscar Barquero-Pérez** received the Technical Telecommunication Engineering Degree from Universidad Carlos III de Madrid, Spain, in 2005. Currently, he is attending a MSc programme in Biomedical Engineering in Universidade do Porto, Portugal, and he is collaborating with Department of Signal Theory and Communications at Universidad Rey Juan Carlos, Spain. His main research interests include linear and nonlinear time series analysis and biomedical signal processing.



**Inmaculada Mora-Jiménez** received the Telecommunication Engineering degree from Universidad Politécnica de Valencia, Spain, in 1998, and the PhD degree from Universidad Carlos III de Madrid, Spain, in 2004. Currently, she is an Associate Professor in the Department of Signal Theory and Communications at Universidad Rey Juan Carlos, Spain. Her main research interests include statistical learning theory, neural networks, and their applications to image processing, bioengineering, and communications.



**Estrella Everss** was born in Valencia, Spain. She obtained the BA Degree (1995) and the PhD (2003) in Psychology from Universitat de Valencia, Spain. Since 2003, she was a postdoctoral researcher at the Universidad Carlos III de Madrid, Spain, and in 2007 she joined the Department of Signal Theory and Communications in Universidad Rey Juan Carlos, Spain. Her research is mainly devoted to biomedical signal analysis and processing.



**Ana Belén Rodríguez-González** was born in Plasencia (Cáceres), Spain. She received her BS degree in Telecommunication Engineering in 2000 from Universidad de Valladolid, Spain, and her BA degree in Economics in 2002 from Universidad Nacional de Educación a Distancia (UNED), Spain. She was an Assistant Professor at the Department of Signal Theory and Communications, Universidad Carlos III de Madrid, Spain, where she began her PhD. In 2007 she joined the Department of Signal Theory and Communications, Universidad Rey Juan Carlos, Madrid, Spain, where she currently develops her research and teaching activities as an Assistant Professor. Her research interests include P2P networks, multi-agents systems, and statistical signal processing.



**Arcadi García-Alberola** received the MD (1982) and the PhD (1991) from Universitat de Valencia, Spain. Since 1993 he has been a Cardiologist and an Professor of Medicine at Hospital Universitario Virgen de la Arrixaca and Universidad de Murcia, where he is the Chief of the Laboratory of Cardiac Electrophysiology. He has co-authored more than 120 scientific papers and more than 50 communications in cardiac electrophysiology, and his main research areas are repolarization analysis, arrhythmia mechanisms, and cardiac signal processing.